

A Dual Receptor Cross-talk Model of G protein-coupled Signal Transduction

Running Head: Dual Receptor GPCR Crosstalk Model

Patrick Flaherty<sup>1</sup>, Mala L. Radhakrishnan<sup>2</sup>, Tuan Dinh<sup>3</sup>, Michael I. Jordan<sup>4</sup>, Adam P.

Arkin<sup>5\*</sup>

<sup>1</sup>Department of Electrical Engineering and Computer Sciences, UC Berkeley, Berkeley,  
CA, 94720

<sup>2</sup>Department of Chemistry, Computer Science and Artificial Intelligence Laboratory,  
Massachusetts Institute of Technology, Cambridge, MA 02139

<sup>3</sup>Department of Bioengineering, UC Berkeley, Berkeley, CA, 94720

<sup>4</sup>Department of Statistics and Computer Science Division, UC Berkeley, Berkeley, CA  
94720

<sup>5</sup> Physical Biosciences Division, Lawrence Berkeley Laboratory, Howard Hughes  
Medical Institute, Department of Bioengineering, UC Berkeley, Berkeley, CA 94720

\*Corresponding Author: Adam P. Arkin, 717 Potter Street, Berkeley, CA, 94710,  
V: (510) 495-2366, F: (510) 486-6219, aparkin@lbl.gov

Number of text pages: **16**

Number of figures: **5**

Number of tables: **1**

Number of words in the abstract: **216**

Number of characters in the paper: **44,725**

Macrophage cells that are stimulated by two different ligands that bind to G protein-coupled receptors (GPCRs) usually respond as if the stimulus effects are additive, but for a minority of ligand combinations the response is synergistic. The G protein-coupled receptor system integrates signaling cues from the environment to actuate cell morphology, gene expression, ion homeostasis and other physiological states. We analyze the effects of the two signaling molecules complement factor 5a (C5a) and uridine diphosphate (UDP) on the intracellular second messenger calcium to elucidate the principles that govern the processing of multiple signals by G protein-coupled receptors. We have developed a formal hypothesis, in the form of a kinetic model, for the mechanism of action of this GPCR signal transduction system using data obtained from RAW264.7 macrophage cells. Bayesian statistical methods are employed to represent uncertainty in both data and model parameters and formally tie the model to experimental data. When the model is also exploited as a tool in the design of experiments, it predicts a synergistic region in the calcium peak height dose response that results when cells are simultaneously stimulated by C5a and UDP. An analysis of the model reveals a potential mechanism for crosstalk between the G $\alpha$ i-coupled C5a receptor and the G $\alpha$ q-coupled UDP receptor signaling systems that results in synergistic calcium release.

## Background

The G protein-coupled signal transduction system integrates a wide range of intercellular signals and actuates downstream pathways. G protein-coupled receptors (GPCRs) are composed of seven  $\alpha$ -helices that span the plasma membrane, an extracellular domain that is activated by an agonist and an intracellular domain that binds a guanine nucleotide heterotrimer made up of different  $\alpha$ ,  $\beta$  and  $\gamma$  subunit isoforms. This receptor system accounts for 40-50% of modern medicinal drug targets but only 10% of the known receptors are targeted by drugs (Kroeze et al.). Though the system is physiologically and pharmacologically important, the mechanism by which the system integrates multiple signals is not well understood (Werry et al.).

We address the G-protein mediated route to calcium release in RAW264.7 cells. When activated by a specific ligand, the G protein heterotrimer dissociates to free  $G\alpha$ -GTP and  $G\beta\gamma$ . Specific  $G\alpha$  and  $G\beta\gamma$  isoforms are able to bind specific isoforms of phospholipase C  $\beta$  (PLC $\beta$ ) and catalyze the synthesis of inositol (1,4,5)-triphosphate (IP3) and diacylglycerol (DAG) from phosphatidylinositol (4,5)-bisphosphate (PIP2). In addition to its catalytic activity, PLC $\beta$  acts as a GTPase for  $G\alpha$ -GTP. IP3 binds to specific receptor-channels on the membrane of the ER to release  $Ca^{2+}$  into the cytosol. DAG and  $Ca^{2+}$  bind to and activate protein kinase C (PKC) which may phosphorylate and inactivate specific PLC $\beta$  isoforms. G protein receptor kinase (GRK) is activated once it is phosphorylated by PKC (Penela et al.) and is localized to the plasma membrane by  $G\beta\gamma$  (Pitcher et al.). Though phosphorylation has not been shown to be necessary for GRK activation, we have assumed so in our model because phosphorylation by PKC may release the inhibition of GRK2 by being bound to calmodulin (Penela et al.). Activated GRK can then phosphorylate specific GPCRs which leads to receptor inactivation – perhaps directly or by arrestin activity. In this complex signal transduction network,  $G\alpha$  and  $G\beta\gamma$  subunits have different patterns of specificity for PLC $\beta$  isoforms and calcium is an important cofactor in several important feedback loops (Berg et al. 2002).

The two extracellular signaling ligands we consider here are C5a and UDP. The small peptide C5a is potent anaphylotoxin and a strong chemoattractant for many immune system components (Allegretti et al.). The calcium response due to stimulation by C5a is predominantly coupled through  $G\alpha i$ -linked heterotrimers. Macrophage cells and their precursors, monocytes, express several receptors that are specific to extracellular nucleotides and it has been shown that the P2Y6 receptor, which is sensitive to UDP, regulates the production and secretion of the chemokine interleukin 8 (IL-8) in monocytes (Warny et al.). The UDP response is mediated by  $G\alpha q$ -linked heterotrimers, but other receptors in the P2Y family may respond to UDP and couple the signal through other G protein isoforms.

Four recent models have sought to explore various aspects of the G protein coupled signal transduction system in detail. Lukas et al. compare measured calcium response over a range of bradykinin doses to their model predictions (Lukas 2004). Mishra &

Bhalla built a model to investigate the role of IP4 as a signal coincidence detector in the GPCR pathway (Mishra and Bhalla). The model by Lemon et al. predicts the calcium response to UTP stimulation and is the closest in focus to our model (Lemon et al.). A recent model of calcium dynamics in RAW cells has been proposed that is quite similar to this model, but does not deal with crosstalk between receptors or formal statistical uncertainty in model predictions (Maurya and Subramaniam 2007b, 2007a).

Several hypotheses for the mechanism of crosstalk and synergy among GPCR-mediated pathways have been proposed. Cross-talk among GPCR-mediated pathways is important both physiologically and pharmaceutically. Quitterer et al. propose that crosstalk is mediated by G $\beta\gamma$  exchange between G $\alpha i$ -coupled and G $\alpha q$ -coupled receptors (Quitterer and Lohse 1999). Zhu et al. speculated that PLC is under either conditional or dual regulation of G $\beta\gamma$  and G $\alpha$  (Zhu and Birnbaumer 1996). Though these hypothetical mechanisms for crosstalk among G protein coupled receptor systems are conceptually plausible we have not found these or any other of the many competing hypothetical mechanisms tested in the context of a quantitative mathematical model (Werry et al. 2003).

In this paper Bayesian statistical inference is used to provide a rigorous connection between the mathematical model derived from mass-action kinetics, prior information from in-vitro biochemical studies and heterogeneous experimental data. The prior distribution over the parameters represents our uncertainty before observing a set of experimental data. A broad, high variance, prior distribution means we are quite uncertain and a concentrated, low variance, prior means we are more certain about the parameter a priori. The objective of our inference is the posterior distribution over the parameters because it is an informed estimate of both the value of the parameter and the uncertainty in the parameter value. The posterior distribution over the parameters is then used as a tool for experiment design to estimate the model-based posterior distribution over observable quantities such as the cytosolic calcium concentration and to drive the design of new experiments. This statistical approach is possible in a model of this size because of the abundance and quality of the data collected for this study.

## Model Structure

There are two main features of the structure of our model, shown in Figure 1, which contribute to crosstalk in the system and produce the key dynamical features in the calcium response: isoform specificity and calcium-dependent feedback. As we will show, by including multiple isoforms of PLC $\beta$  and G $\alpha$  as well as the negative feedback mediated by PKC, GRK and the IP3 receptor itself, we are able to predict the synergistic interaction between C5a and UDP observed in the experimental data.

### [FIGURE 1 HERE]

Our representation of the G protein-coupled signal transduction system includes C5a and P2Y6 receptors, G $\alpha i 2$ , G $\alpha q$ , G $\beta\gamma$ , PLC $\beta 3$ , PLC $\beta 4$ , PIP2, DAG, IP3, PKC, GRK2, calcium buffer, a Na $^{2+}$ /Ca $^{2+}$  exchanger, a sarco(endo)plasmic reticulum Ca $^{2+}$ -ATPase (SERCA) pump, IP3 receptors and RGS. The model is composed of 53 coupled ordinary

differential equations with 84 parameters and 24 non-zero initial conditions. The complete model equations are shown in Figure S7 (supplementary information). The parameters and initial conditions are in Table S2 and Table S1 respectively (supplementary information). Where available, we have relied on *in-vitro* or *in-vivo* biochemical experiments for the reactions and parameter values (see supplementary information). In cases where the biochemical parameter values were not known, we chose physically reasonable values. Twenty of the 84 parameters most relevant to the knock-down and wild-type data were estimated from cytosolic calcium measurements as described in the Methods section. Most reactions were assumed to be governed by mass-action kinetics, but for a few proteins – such as RGS – the mechanism of regulation is not known in enough detail and we have approximated with Michaelis-Menten kinetics or a phenomenological function.

We briefly discuss the reactions involving the  $\text{Na}^{2+}/\text{Ca}^{2+}$  exchanger, SERCA pump, IP3 receptors, RGS and calcium buffer because they are important for the faithful representation of the system in our model. Regulators of G protein signaling (RGS) are GTPase proteins that down-regulate the extent of signaling (Kehrl 1998); RGS2 at least is expressed in RAW264.7 macrophage cells and therefore an RGS activity is included in our model. The mechanism of activation of RGS2 as it relates to  $\text{G}\alpha_i$  and  $\text{G}\alpha_q$  signaling is not entirely known and is difficult to assess because antibodies that specifically recognize RGS2 are not widely available (Ross and Wilkie 2000; Cunningham et al. 2001; Kehrl and Sinnarajah 2002). We have assumed constitutive activity and expect as more information becomes available a more accurate model of the regulation of RGS2 and other RGS isoforms will be possible. The SERCA pump helps to bring the cytosolic  $\text{Ca}^{2+}$  concentration back to the resting level after stimulation. We have modeled the SERCA pump as in the Keizer and DeYoung model (Keizer and De Young 1992). The IP3 dependent opening of ER calcium channels was found to be cooperative (Meyer et al. 1988) and we have used the Meyer and Stryer model for the IP3-gated channel with a Hill coefficient of four (Meyer and Stryer 1988; Keizer and De Young 1992). Finally, many other proteins such as calmodulin and the fluorescent indicator Fura-2 bind  $\text{Ca}^{2+}$ . Because our measurements reflect these effects, we have included a general buffer for cytosolic calcium.

## Isoform Specificity

Complement factor 5a activates the C5a receptor which is a  $\text{G}\alpha_i$ -coupled receptor (Jiang et al. 1996). The released  $\text{G}\beta\gamma$  dimer activates PLC $\beta 2$  and PLC $\beta 3$  which are lumped and called PLC $\beta 3$  in our model because: (i) the activity of  $\text{G}\beta\gamma$ -activated PLC $\beta 3$  has been shown to be greater than  $\text{G}\beta\gamma$ -activated PLC $\beta 2$  in *in-vitro* studies and (ii)  $\text{G}\alpha_q$  activates both PLC $\beta 2$  and PLC $\beta 3$  so the structural connections from  $\text{G}\beta\gamma$  and  $\text{G}\alpha_q$  to PLC $\beta 2$  and PLC $\beta 3$  in the model are identical (Park et al. 1993; Wu et al. 1993). PLC $\beta 1$  is activated by  $\text{G}\beta\gamma$  and  $\text{G}\alpha_q$ , but RAW264.7 macrophage cells do not express this isoform, so we have not included it in the model. PLC $\beta 3$  then catalyzes the hydrolysis of phosphatidylinositol (4,5)-bisphosphate (PIP2) into inositol 1,4,5-trisphosphate (IP3) diacylglycerol (DAG).

UDP stimulates the P2Y6 receptor and the associated G $\alpha$ q-GTP activates both PLC $\beta$ 3 (Smrcka and Sternweis 1993) and PLC $\beta$ 4 (Lee et al. 1994). The GTPase rate of G $\alpha$ q is increased 1000-fold when bound to PLC $\beta$  (Mukhopadhyay and Ross 1999). Due to this rapid hydrolysis rate, we have assumed, in our model, that PLC $\beta$ 3 or PLC $\beta$ 4 bound G $\alpha$ q-GTP may only hydrolyze one molecule of PIP2 before releasing G $\alpha$ q-GDP. Additionally, the G $\beta\gamma$  released by the P2Y6 receptor also activates PLC $\beta$ 3 (Smrcka and Sternweis 1993), but does not activate PLC $\beta$ 4 (Jiang et al. 1994).

Our model assumes that PLC $\beta$ 3 does not simultaneously bind G $\beta\gamma$  and G $\alpha$ q. Indeed, a biochemical study of PLC $\beta$ 2 activity in reconstituted membrane fractions strongly argues that G $\alpha$ q and G $\beta\gamma$  do not simultaneously bind this effector (Runnels and Scarlata 1999). While this was specifically demonstrated for PLC $\beta$ 2, we implicitly assume the same holds for PLC $\beta$ 3 because we lump the two in our model. This is a mechanistic assumption of our model and an interesting issue for future testing with directed experiments.

### Calcium-dependent Feedback

Though important for response specificity, the dynamical control of calcium release is not limited to the forward pathway in this system. Calcium participates in feedback processes that both enhance and inhibit its own release at multiple points in the pathway. There are four main nodes of calcium-dependent feedback control in our model: PLC $\beta$ , IP3 receptor, protein kinase C (PKC) and G protein receptor kinase (GRK).

Calcium enhances its own release by binding to the EF-hand domain on PLC $\beta$  and is required for PLC $\beta$  to hydrolyze PIP2 into IP3 and DAG (Rhee 2001). Because the dissociation constant for PLC $\beta$ -Ca $^{2+}$  in our model is larger than the basal concentration of cytosolic calcium, as more Ca $^{2+}$  is released from the ER, more PLC $\beta$ -Ca $^{2+}$  becomes available to bind G $\alpha$ q or G $\beta\gamma$ . This positive feedback mechanism accelerates the release of Ca $^{2+}$ .

In our model, Ca $^{2+}$  and IP3 cooperatively open the channel between the ER and the cytosol. It is believed that Ca $^{2+}$  initially stimulates the IP3 receptor with maximal stimulatory effect at 100-300nM (Patterson et al. 2004). At higher concentrations, Ca $^{2+}$  has an inhibitory effect. We use the IP3 receptor model structure in the Keizer and De Young model for this component (Keizer and De Young 1992).

Protein kinase C (PKC) has been shown to phosphorylate PLC $\beta$ 3 which inhibits PLC $\beta$ 3 activation due to G $\alpha$ q and G $\beta\gamma$  (Yue et al.; Litosch 2002). PKC is activated when bound to DAG and Ca $^{2+}$  (Ananthanarayanan et al. 2003; Spitaler and Cantrell 2004). Because the preferred order of binding is not entirely known, PKC, DAG and Ca $^{2+}$  form a thermodynamic cycle of reversible reaction with only the PKC-DAG-Ca $^{2+}$  form active. In our model, the dissociation constant of PKC and Ca $^{2+}$  is much greater than the basal Ca $^{2+}$  concentration, and upon binding DAG, the PKC-DAG complex has a higher affinity for Ca $^{2+}$  making the order of binding preferentially PKC to DAG then PKC-DAG to Ca $^{2+}$ .

It is not known whether PLC $\beta$ 4 is also regulated by PKC. We have assumed, in our model, the same mechanism of PKC regulation of PLC $\beta$ 3 and PLC $\beta$ 4.

The final key calcium-dependent feedback loop in our model is mediated by G protein receptor kinase (GRK). GRK2 phosphorylates and inactivates ligand-bound C5a receptors when activated by PKC and G $\beta$  $\gamma$ . In sequence, PKC phosphorylates GRK2 which causes translocation to the plasma membrane (Penela et al. 2003). When properly localized, GRK2 may bind G $\beta$  $\gamma$  and then phosphorylate the C5a-C5a receptor complex to inactivate it (Langkabel et al. 1999). This simplified representation of the receptor desensitization mechanism does not include arrestin activity, multiple receptor phosphorylation sites and other fine grain or slower biochemical interactions that may be present *in-vivo*.

## Single Ligand Experiments

Having specified the structure of our model, we direct our attention to the parameters. We estimate 20 of the 84 parameters in our model using a data set composed of 96 Fura-2 time series measurements as described in the Materials and Methods section. Each experiment consists of 3-4 samples from different wells in a 96 well plate. There are 15 experiments spanning 9 doses of C5a and 14 experiments spanning 11 doses of UDP on wild-type cells in the data set. The data set also contains calcium measurements on 5 different shRNAi knockdown cell lines constructed by lentiviral infection. The time interval between samples is approximately 3-4 seconds and each time series is approximately 100-300 seconds of post-stimulation data. Table 1 shows a summary of the knockdown data used for statistical parameter estimation for this model in addition to the wild-type experiments.

### [TABLE 1 HERE]

We find that our model is generally quantitatively consistent with the experimental data within measurement uncertainty. Where the model is less consistent with the data – specifically for the GRK knockdown experiment – we find the deviation has a reasonable biological explanation. The summary of the data set and the fit of the model to each single ligand experiment are available in the supplementary information. We briefly discuss some issues relating to goodness of fit and the Bayesian parameter estimation results here.

While most optimization procedures produce a point estimate of the parameters that maximize the goodness of fit of the model to the observed data, the Bayesian procedure we have employed here estimates the entire posterior distribution of the parameters given the data. This information is valuable for qualitatively and quantitatively evaluating the precision of the parameters estimates. Figure 2 shows, as a qualitative evaluation, that while the a-priori forward and reverse binding rates for the receptors (C5aR and P2YR) are uncorrelated they are correlated in the posterior distribution. The calcium measurements have informed and constrained the posterior estimates of the dissociation

constants to be approximately 5nM and 250nM for the C5aR and P2YR respectively. We have quantitatively computed marginal highest posterior density (HPD) confidence intervals for each of the twenty parameters we have estimated from the data. Those estimates are shown in Table S3. Those parameters with large HPD intervals are not well informed by the measurements and are candidates for directed biochemical experiments.

### [FIGURE 2 HERE]

#### **Wild-type Experiments**

The calcium response to C5a adapts and returns to the basal level, but the UDP response has a sustained elevated calcium level that slowly decays. Figure 3 shows two representative experiments of the response of the wild-type cell to stimulation with C5a and UDP. We expect that the fit to this data will be good because 20 key model parameters were fit using an experimental data set that included these experiments – the fit is indeed accurate. The point estimate curve is constructed from the maximum a-posteriori parameters from an MCMC chain. The prediction intervals are estimated by Monte Carlo sampling from the posterior parameter distribution and the measurement error distribution conditional on the parameters. The prediction confidence intervals generally cover the observed data.

### [FIGURE 3 HERE]

#### **Knockdown Experiments**

Lentiviral infection is used to introduce small hairpin RNAs to interfere with the translation of the key signaling proteins GRK2, G $\alpha$ i2, G $\alpha$ q, PLC $\beta$ 3 and PLC $\beta$ 4 (Shin et al. 2006). There are three main sources of uncertainty in the knockdown experiment model predictions: parametric uncertainty, measurement uncertainty and knockdown efficiency uncertainty. We have dealt with the first two sources in the previous section on wild-type experiments. Here we address prediction variability due to knockdown efficiency uncertainty by using nominal parameter values.

### [FIGURE 4 HERE]

Figure 4 shows simulations and experimental data for three representative knockdown experiments. The upper-left panel of Figure 4 shows a GRK knockdown line stimulated with 250nM C5a. Because GRK2 desensitizes the C5a receptor, we expect that by eliminating the feedback mechanism, the calcium peak will be higher and more sustained. The experimental data as well as the model indeed show that effect. Quantitatively, the model prediction shows a greater effect than the experimental data. A likely reason is that the model only considers one isoform of GRK while there are four isoforms expressed in the RAW264.7 cell line (GRK1,2,4,6). If more than one isoform can desensitize the C5a receptor, the effective knockdown in desensitization function will be less than as measured by western blot analysis on GRK2.

While GRK does not desensitize the P2Y receptor in our model, it is a buffer for G $\beta$  $\gamma$  released from G $\alpha$ q. Reducing the amount of GRK will shift the equilibrium towards

more G $\beta\gamma$  bound to PLC $\beta$ 3 and thus more calcium release even though GRK does not directly feed back on the P2Y6 receptor. The top-right panel in Figure 3 shows that, based on the model, the peak intracellular calcium concentration is expected to be very slightly higher in the GRK2 knockdown line when stimulated by 25 $\mu$ M UDP. A comparison of the experimental peak heights of the wild-type and GRK knockdown cell line data by t-test cannot reject the null hypothesis that the peak heights are equal ( $p=0.9963$ ).. The effect of the GRK knockdown is expected to be so slight that the effect size is overwhelmed by the measurement error in the data. The effect of the uncertainty in the GRK2 knockdown fraction impacts the range of the confidence intervals of the predicted C5a response much more than the confidence intervals of the predicted UDP response which is consistent with GRK2 being a more significant component of the C5a response.

Our model structure has PLC $\beta$ 3 stimulated by either G $\beta\gamma$  or G $\alpha$ q. Because the C5a response signals only through PLC $\beta$ 3 the effect of the knockdown is expected to be more pronounced for the C5a response than for the UDP response. The bottom-left panel of Figure 3 confirms that the model prediction is consistent with the representative experiment. The UDP response activates PLC $\beta$ 3 through G $\beta\gamma$ , but also activates PLC $\beta$ 3 and PLC $\beta$ 4 with G $\alpha$ q. Therefore, we expect that the calcium response should be more robust to perturbations in just one of the PLC $\beta$  isoforms. The UDP response in the PLC $\beta$ 3 knockdown line (bottom right panel of Figure 4) shows that our model predicts the knockdown effect to be small relative to the total magnitude of the response in part due to the redundancy in the use of PLC $\beta$  isoforms in the UDP response.

Because this data set was used for parameter estimation, the fit of model to the data may overstate the accuracy of the model. Nonetheless, the good fit does suggest that the model warrants being tested in truly predictive experiments; we describe such experiments in the following section.

## Double Ligand Experiments

We examine our model response to a simultaneous stimulation by C5a and UDP because it has been shown experimentally that macrophage cells respond synergistically to such conditions. To quantify the amount of synergy or non-additivity that is present in the calcium response, a *synergy ratio* is computed for each ligand dose pair. The numerator of the ratio is the peak offset from baseline of the intracellular calcium concentration. The denominator of the ratio is the sum of the peak offsets when the cell or model is stimulated with only one ligand. A synergy is present when the ratio is greater than one implying the peak height is greater than expected from an additive combination of ligand effects. While this is certainly not the only possible measure of synergy it is widely adopted and has been used in previous studies on calcium synergy (Natarajan et al.).

[FIGURE 5 HERE]

The left panel of Figure 5 shows the results of model simulations at nominal parameters for a grid of doses of C5a and UDP. In the dose response surface, there is a ridge of synergistic calcium release for a moderate dose of UDP. We tested the model prediction with the experiment design measuring the synergy ratio at the points denoted as black open circles in the left panel of Figure 5. A  $\chi^2$  goodness-of fit test comparing the model expected synergy ratio to the observed synergy ratio fails to reject the null hypothesis that the data were generated by the model mechanism ( $p\text{-value} \approx 1.0$ ). The root-mean-squared error (RMSE) deviation between the predicted and actual experimental data is 0.492. By way of comparison, the RMSE between the data and the null model of no synergy is 1.044. We therefore conclude that the model predictions are consistent with the experimental observations. It should be noted that measurements of synergy in RAW cells are noisy and the ridge occurs at low doses of UDP. Notwithstanding, the phenomenon has been reported (Natarajan et al.) and has been observed by us in this cell line.

The right panel of Figure 5 shows the same synergy dose response surface but for a GRK knockdown cell line. The synergy ridge observed in the wild-type cell simulation is changed in the GRK knockdown simulation indicating the C5a receptor desensitization mechanism mediated by GRK is important for the synergistic release of calcium. In the next section we pursue this conclusion in more detail, developing a conceptual explanation of the mechanism of crosstalk and synergy within our model.

## Discussion

G protein-coupled receptors form a complex network of interacting proteins that generally exhibits the properties of a system in which each receptor signal is buffered from the others. For a minority of ligand combinations, however, crosstalk between pairs of receptors is apparent. Due to the complexity and importance of the system many hypothetical mechanisms have been proposed to explain the crosstalk (Werry et al. 2003). In particular, simultaneous G $\beta\gamma$  and G $\alpha q$  binding to PLC $\beta$  (Zhu and Birnbaumer 1996) and G $\beta\gamma$  exchange between G $\alpha i$  and G $\alpha q$ -coupled receptors have been proposed as potential mechanisms (Quitterer and Lohse 1999). While our model does not eliminate these potential mechanisms, we do show that the mechanism represented in our model is consistent with a full range of experimental data including a variety of doses of C5a and UDP, C5a and UDP stimulation of five different knockdown cell-lines and double-ligand dose response experiments.

To our knowledge, this is the first multireceptor GPCR model and the first to address the complex phenomenon of crosstalk between GPCR receptor pathways that has been statistically estimated and validated with experimental data. This important phenomenon plays a role in processes as diverse as chemotaxis and perhaps drug interactions. In our model, the primary mechanism of synergy is due to the cooperative opening of the IP3 receptor. The robustness of the synergy is due to the feedback of GRK on the C5a receptor and the specificity of the synergy is due to the interaction patterns between specific G $\alpha$  isoforms and PLC $\beta$  isoforms. The simultaneous binding model (Zhu and Birnbaumer) accounts for the specificity of synergy, but not the robustness pattern of the synergy.

We observe in the model that if the  $G\alpha q$ -PLC $\beta 3$ -Ca $^{2+}$  and  $G\alpha q$ -PLC $\beta 4$ -Ca $^{2+}$  binding reactions are inhibited, the system still exhibits synergy. We conclude from this observation that the crosstalk mechanism is mediated by G $\beta\gamma$ . If binding reaction of G $\beta\gamma$  to phosphorylated GRK2 is removed, the synergy is eliminated. Furthermore, if the GRK2-mediated phosphorylation of complexed C5a receptors is removed, the double ligand response is additive. We deduce then that the synergy mechanism involves GRK2 phosphorylation of complexed C5a receptors. However, GRK2 phosphorylation does not entirely explain the synergy mechanism.

In our model, the calcium released from the IP3 receptor is a function of the number of receptor molecules complexed to IP3 raised to the fourth power (De Young and Keizer 1992). Therefore, for a small range of IP3 concentration, the amount of Ca $^{2+}$  released is more than additive (see Figure S8, supplementary information). We conclude from our analysis of the model that the synergy ridge in Figure 4 arises because the GRK2 mediated mechanism holds the IP3 concentration in this non-additive region for most concentrations of C5a. The UDP response does not have the GRK2 mediated feedback and thus only shows a synergistic response for a small range of UDP concentration. If the GRK2 desensitization is removed from the model, the synergy ridge is removed and synergy is only present at low doses of C5a and UDP (see Figure 5).

The Bayesian method we have used for this model has several advantages for the estimation of model parameters in complex mechanistic system models. We have used an informative prior to exclude negative rate constants from the permitted parameter space. We have also used the prior distribution to center our a priori expectations of the true rate constant at values obtained from *in-vitro* and other biochemical experiments. The Bayesian update rule allowed us to estimate parameters with our best current data set and then update those estimates as new data became available from the calcium assay. In this way, we were able to iteratively refine and recalibrate our model with the most recent data available during data collection period for this project. The posterior distribution provides not only an estimate of the rate constants, but the entire distribution, from which we can calculate highest posterior confidence intervals and posterior correlations between parameters. For example, the posterior correlation between the binding and unbinding rates for the UDP-P2Y receptor complex were highly correlated, but those two constants were uncorrelated with the corresponding rates for the C5a-C5a receptor complex reaction even though we imposed no correlations a priori. Finally, the algorithmic methods for collecting ensembles of samples from the posterior distribution have improved considerably in recent years in terms of speed and robustness

We have shown that the signal transduction system as it is represented by our model does not require simultaneous binding of  $G\alpha q$  and G $\beta\gamma$  to PLC $\beta 3$  to cause a synergistic Ca $^{2+}$  response due to simultaneous stimulation by C5a and UDP. We have shown that our representative model is consistent with this experimental data set in RAW264.7 macrophage cells, but we have not excluded all other potential mechanisms that may be absent or regulated differently in this cell line compared to other macrophage cell lines.

Indeed there are a few examples of statistical discrepancies between the model and experiments in our data set (Table S4). These differences are substrate for further experimentation and modeling. The purpose of our model is to provide a quantitative tool to aid in reasoning about such complex interacting systems so that meaningful experiments can be designed to explore and understand the biological mechanism.

## **Materials and Methods**

The model equations are given in Figure S7 of the supplementary information. The initial conditions and parameter values are in Tables S1 and S2 respectively. All the data used in this work and a stand-alone implementation of the model is provided at <http://genomics.lbl.gov/supplemental/flaherty-gpcr/>. The model was simulated using CVODE (Hindmarsh et al. 2005) and the GNU Scientific Library. Further details on materials and methods are available in supplementary information.

## ***Experimental Methods***

Intracellular free calcium in cultured adherent RAW264.7 cells was measured in a 96-well plate format using the  $\text{Ca}^{2+}$ -sensitive fluorescent dye Fura-2 (Grynkiewicz et al.; Tsien). A Molecular Devices FLEXstation scanning fluorometer was used to measure fluorescence using a bottom read of a 96-well plate. Each well was sampled approximately every 4 seconds. The measurement protocol is described in AfCS experimental protocol ID #PP00000211 (available from <http://www.signaling-gateway.org>). The parameters in ligand concentration model were estimated using FITC solution in the FLEXstation scanning fluorometer as described in Molecular Devices Maxline Application Note #45 and in Protocol #1 in the supplementary information.

## ***Statistical Inference***

Twenty of the 84 parameters were chosen to be estimated from data based on relevance to the experimental hypothesis. Only those parameters that related to the knockdown experiments in the data set were estimated and are denoted with a star in Table S2. We used data to estimate only the two forward rate constants in the enzymatic mass-action equations because the forward and reverse rate constants for a given reaction will be highly correlated in the posterior distribution making estimation by Markov chain methods computationally expensive.

For each estimated parameter we constructed an independent Gaussian prior on a log scale with a mean chosen based on relevant literature and a standard deviation of 0.25. We found that this prior variance was sufficiently permissive to allow exploration of the space while still constraining the rates to be physically reasonable. The prior distribution over the parameters allows the incorporation of both soft and hard constraints in the parameter estimates. Parameter sets with zero measure are not permitted in the posterior distribution and parameter sets with small measure must be assigned a large likelihood in order to have a large posterior probability.

The likelihood is a function of the parameters ( $\theta$ ) and links the prior distribution with the posterior distribution under Bayes rule

$$\Pr(\theta | y) = \frac{p(y | \theta) \Pr(\theta)}{\Pr(y)}$$

where  $y$  denotes the observed data.

In our model, the likelihood function is a Gaussian distribution according to the non-linear regression equation  $y = f(\theta) + \varepsilon$ ,  $\varepsilon \sim N(0, \sigma^2)$ , where  $f(\theta)$  is the deterministic model prediction. The posterior distribution is of interest because it informs us as to the most probable setting of the parameters as well as the uncertainty in the values.

The Metropolis-Hastings algorithm (Robert and Casella 2004) was used to estimate the posterior density of the parameters  $\Pr(\theta|y)$ . Three independent chains were simulated from different initial parameter values. To assess convergence of the posterior distribution estimate, we used the Gelman-Rubin potential scale reduction factor (PSRF) (Gelman and Rubin 1992). The multivariate PSRF is 2.44 and 95% of the individual PSRFs were less than 1.5. A PSRF value of one indicates that the distribution has converged and values near one are close to converged.

Posterior prediction confidence intervals were constructed using the percentiles from the predictive distribution approximated with 2000 Monte Carlo samples from  $\Pr(y_{\text{new}} | \theta_i)$  at each of 100 simple random samples from  $\Pr(\theta | y)$  obtained from

$$\Pr(y_{\text{new}} | y) = \int \Pr(y_{\text{new}} | \theta) \Pr(\theta | y) d\theta \approx \sum_{i=1}^{100} \Pr(y_{\text{new}} | \theta_i) \Pr(\theta_i | y),$$

where  $\Pr(y_{\text{new}} | \theta_i) \sim N(f(\theta), s^2)$  and  $s^2$  is the pooled variance estimate, which is computed as an average of the variances of all the time points in each of the 29 wild-type experiments. These average variances were weighted by the number of technical replicates in each experiment and then averaged to yield the estimate  $s^2$ . A small factor of  $1nM^2$  was added to each variance estimate to bound variance estimates away from zero.

## Acknowledgements

PF, APA and MIJ designed the research. PF and MLR performed the research. PF and TD analyzed the data. PF, MIJ and APA wrote the paper. The authors would like to thank William Seaman, Robert Rebres, Tamara Roach, Mel Simon and the Alliance for Cellular Signaling for the experimental data used in this study and many informative and interesting conversations. MLR was supported by a Department of Energy Computational Science Graduate Fellowship (DOE CSGF, DE-FG02-97ER25308). PF, TD and APA were supported by the Alliance for Cellular Signaling (NIH: U54 GM62114). APA would also like to acknowledge support of the Howard Hughes Medical Institute. MIJ was supported by a grant from Microsoft Research and a grant from Yahoo! Research.

Table 1:

The data set used for parameter estimation is shown in this table. Five different cell lines that have a perturbation in the level of a key signal transduction protein were constructed by shRNAi lentiviral infection. The calcium response from these cell lines in addition to the wild-type cell line were used to fit relevant parameters in the model. Because shRNAi does not entirely remove the protein product, the fraction knockdown was estimated by qRT-PCR and by Western blot analysis. The standard error (se) was computed for each estimate and the upper and lower confidence intervals were computed as  $\pm 3 \cdot se$ . The knockdown confidence intervals are used in the GPCR model to construct prediction confidence intervals for the calcium response. Where several cell lines were constructed for each knockdown, the best was selected and reported in parenthesis. The sample size for each knockdown-ligand dose combination is shown in the last 6 columns.

Table 1:

Cell Line	Measured Fraction			Sample Size						
	Knockdown		Model Value			C5a			UDP	
	qRT-PCR	Western	Nominal	Lower	Upper	<10nM	10 - 100nM	>100nM	<1μM	1 - 10μM
Wild-type	-	-	-	-	-	4	8	3	5	5
GRK2 (2)	90% ± 7%, n=5	40% ± 6%, n=6	40.0%	22.0%	58.0%	2	12	2	3	1
	83% ± 5%, n=4	73% ± 6%, n=5	73.0%	55.0%	91.0%	-	5	-	5	-
Gai2 (3)	70% ± 8%, n=7	66% ± 23%, n=2	66.0%	0.0%	95.0%	-	3	-	1	-
	83% ± 15%, n=3	-	83.0%	38.0%	100.0%	-	3	-	-	3
PLCb3 (1)	-	87% ± 6%, n=5	87.0%	69.0%	100.0%	-	4	-	4	-
PLCb4 (1)	-	-	-	-	-	-	-	-	-	4

## References

- Allegretti M, Moriconi A, Beccari AR, Di Bitondo R, Bizzarri C et al. (2005) Targeting C5a: recent advances in drug discovery. *Curr Med Chem* 12(2): 217-236.
- Ananthanarayanan B, Stahelin RV, Digman MA, Cho W (2003) Activation mechanisms of conventional protein kinase C isoforms are determined by the ligand affinity and conformational flexibility of their C1 domains. *J Biol Chem* 278(47): 46886-46894.
- Berg JM, Tymoczko JL, Stryer L, National Center for Biotechnology Information (U.S.) (2002) Biochemistry. Available: <http://www.ncbi.nlm.nih.gov/books/bv.fcgi?call=bv.View..ShowTOC&rid=stryer.TOC&depth=2>.
- Cunningham ML, Waldo GL, Hollinger S, Hepler JR, Harden TK (2001) Protein kinase C phosphorylates RGS2 and modulates its capacity for negative regulation of Galphai 11 signaling. *J Biol Chem* 276(8): 5438-5444.
- De Young GW, Keizer J (1992) A single-pool inositol 1,4,5-trisphosphate-receptor-based model for agonist-stimulated oscillations in Ca<sup>2+</sup> concentration. *Proceedings of the National Academy of Sciences of the United States of America* 89(20): 9895-9899.
- Gelman A, Rubin DB (1992) Inference from Iterative Simulation Using Multiple Sequences. *Statistical Science* 7(4): 457-472.
- Grynkiewicz G, Poenie M, Tsien RY (1985) A new generation of Ca<sup>2+</sup> indicators with greatly improved fluorescence properties. *J Biol Chem* 260(6): 3440-3450.
- Hindmarsh AC, Brown PN, Grant KE, Lee SL, Serban R et al. (2005) SUNDIALS: Suite of Nonlinear and Differential/Algebraic Equation Solvers. *ACM Transactions on Mathematical Software* 31(3): 363-396.
- Jiang H, Wu D, Simon MI (1994) Activation of phospholipase C beta 4 by heterotrimeric GTP-binding proteins. *J Biol Chem* 269(10): 7593-7596.
- Jiang H, Kuang Y, Wu Y, Smrcka A, Simon MI et al. (1996) Pertussis toxin-sensitive activation of phospholipase C by the C5a and fMet-Leu-Phe receptors. *J Biol Chem* 271(23): 13430-13434.
- Kehrl JH (1998) Heterotrimeric G protein signaling: roles in immune function and fine-tuning by RGS proteins. *Immunity* 8(1): 1-10.
- Kehrl JH, Sinnarajah S (2002) RGS2: a multifunctional regulator of G-protein signaling. *Int J Biochem Cell Biol* 34(5): 432-438.
- Keizer J, De Young GW (1992) Two roles of Ca<sup>2+</sup> in agonist stimulated Ca<sup>2+</sup> oscillations. *Biophys J* 61(3): 649-660.
- Kroeze WK, Sheffler DJ, Roth BL (2003) G-protein-coupled receptors at a glance. *J Cell Sci* 116(Pt 24): 4867-4869.
- Langkabel P, Zwirner J, Oppermann M (1999) Ligand-induced phosphorylation of anaphylatoxin receptors C3aR and C5aR is mediated by "G protein-coupled receptor kinases. *Eur J Immunol* 29(9): 3035-3046.
- Lee CW, Lee KH, Lee SB, Park D, Rhee SG (1994) Regulation of phospholipase C-beta 4 by ribonucleotides and the alpha subunit of Gq. *J Biol Chem* 269(41): 25335-25338.

- Lemon G, Gibson WG, Bennett MR (2003) Metabotropic receptor activation, desensitization and sequestration-I: modelling calcium and inositol 1,4,5-trisphosphate dynamics following receptor activation. *J Theor Biol* 223(1): 93-111.
- Litosch I (2002) Novel mechanisms for feedback regulation of phospholipase C-beta activity. *IUBMB Life* 54(5): 253-260.
- Lukas TJ (2004) A signal transduction pathway model prototype I: From agonist to cellular endpoint. *Biophys J* 87(3): 1406-1416.
- Maurya MR, Subramaniam S (2007a) A Kinetic Model for Calcium Dynamics in RAW 264.7 Cells: 1. Mechanisms, Parameters and Sub-populational Variability. *Biophys J*.
- Maurya MR, Subramaniam S (2007b) A Kinetic Model for Calcium Dynamics in RAW 264.7 Cells: 2. Knockdown Response and Long-Term Response. *Biophys J*.
- Meyer T, Stryer L (1988) Molecular model for receptor-stimulated calcium spiking. *Proc Natl Acad Sci U S A* 85(14): 5051-5055.
- Meyer T, Holowka D, Stryer L (1988) Highly cooperative opening of calcium channels by inositol 1,4,5-trisphosphate. *Science* 240(4852): 653-656.
- Mishra J, Bhalla US (2002) Simulations of inositol phosphate metabolism and its interaction with InsP(3)-mediated calcium release. *Biophys J* 83(3): 1298-1316.
- Mukhopadhyay S, Ross EM (1999) Rapid GTP binding and hydrolysis by G(q) promoted by receptor and GTPase-activating proteins. *Proc Natl Acad Sci U S A* 96(17): 9539-9544.
- Natarajan M, Lin KM, Hsueh RC, Sternweis PC, Ranganathan R (2006) A global analysis of cross-talk in a mammalian cellular signalling network. *Nat Cell Biol* 8(6): 571-580.
- Park D, Jhon DY, Lee CW, Lee KH, Rhee SG (1993) Activation of phospholipase C isoforms by G protein beta gamma subunits. *J Biol Chem* 268(7): 4573-4576.
- Patterson RL, Boehning D, Snyder SH (2004) Inositol 1,4,5-trisphosphate receptors as signal integrators. *Annu Rev Biochem* 73: 437-465.
- Penela P, Ribas C, Mayor F, Jr. (2003) Mechanisms of regulation of the expression and function of G protein-coupled receptor kinases. *Cell Signal* 15(11): 973-981.
- Pitcher JA, Touhara K, Payne ES, Lefkowitz RJ (1995) Pleckstrin homology domain-mediated membrane association and activation of the beta-adrenergic receptor kinase requires coordinate interaction with G beta gamma subunits and lipid. *J Biol Chem* 270(20): 11707-11710.
- Quitterer U, Lohse MJ (1999) Crosstalk between Galphai(i)- and Galphaq-coupled receptors is mediated by Gbetagamma exchange. *Proc Natl Acad Sci U S A* 96(19): 10626-10631.
- Rhee SG (2001) Regulation of phosphoinositide-specific phospholipase C. *Annu Rev Biochem* 70: 281-312.
- Robert CP, Casella G (2004) Monte Carlo statistical methods. New York: Springer. xxx, 645 p.
- Ross EM, Wilkie TM (2000) GTPase-activating proteins for heterotrimeric G proteins: regulators of G protein signaling (RGS) and RGS-like proteins. *Annu Rev Biochem* 69: 795-827.

- Runnels LW, Scarlata SF (1999) Determination of the affinities between heterotrimeric G protein subunits and their phospholipase C-beta effectors. *Biochemistry* 38(5): 1488-1496.
- Shin KJ, Wall EA, Zavzavadjian JR, Santat LA, Liu J et al. (2006) A single lentiviral vector platform for microRNA-based conditional RNA interference and coordinated transgene expression. *Proc Natl Acad Sci U S A* 103(37): 13759-13764.
- Smrcka AV, Sternweis PC (1993) Regulation of purified subtypes of phosphatidylinositol-specific phospholipase C beta by G protein alpha and beta gamma subunits. *J Biol Chem* 268(13): 9667-9674.
- Spitaler M, Cantrell DA (2004) Protein kinase C and beyond. *Nat Immunol* 5(8): 785-790.
- Tsien RY (1989) Fluorescent indicators of ion concentrations. *Methods Cell Biol* 30: 127-156.
- Warny M, Aboudola S, Robson SC, Sevigny J, Communi D et al. (2001) P2Y(6) nucleotide receptor mediates monocyte interleukin-8 production in response to UDP or lipopolysaccharide. *J Biol Chem* 276(28): 26051-26056.
- Werry TD, Wilkinson GF, Willars GB (2003) Mechanisms of cross-talk between G-protein-coupled receptors resulting in enhanced release of intracellular Ca<sup>2+</sup>. *Biochem J* 374(Pt 2): 281-296.
- Wu D, Katz A, Simon MI (1993) Activation of phospholipase C beta 2 by the alpha and beta gamma subunits of trimeric GTP-binding protein. *Proc Natl Acad Sci U S A* 90(11): 5297-5301.
- Yue C, Ku CY, Liu M, Simon MI, Sanborn BM (2000) Molecular mechanism of the inhibition of phospholipase C beta 3 by protein kinase C. *J Biol Chem* 275(39): 30220-30225.
- Zhu X, Birnbaumer L (1996) G protein subunits and the stimulation of phospholipase C by Gs-and Gi-coupled receptors: Lack of receptor selectivity of Galpha(16) and evidence for a synergic interaction between Gbeta gamma and the alpha subunit of a receptor activated G protein. *Proc Natl Acad Sci U S A* 93(7): 2827-2831.

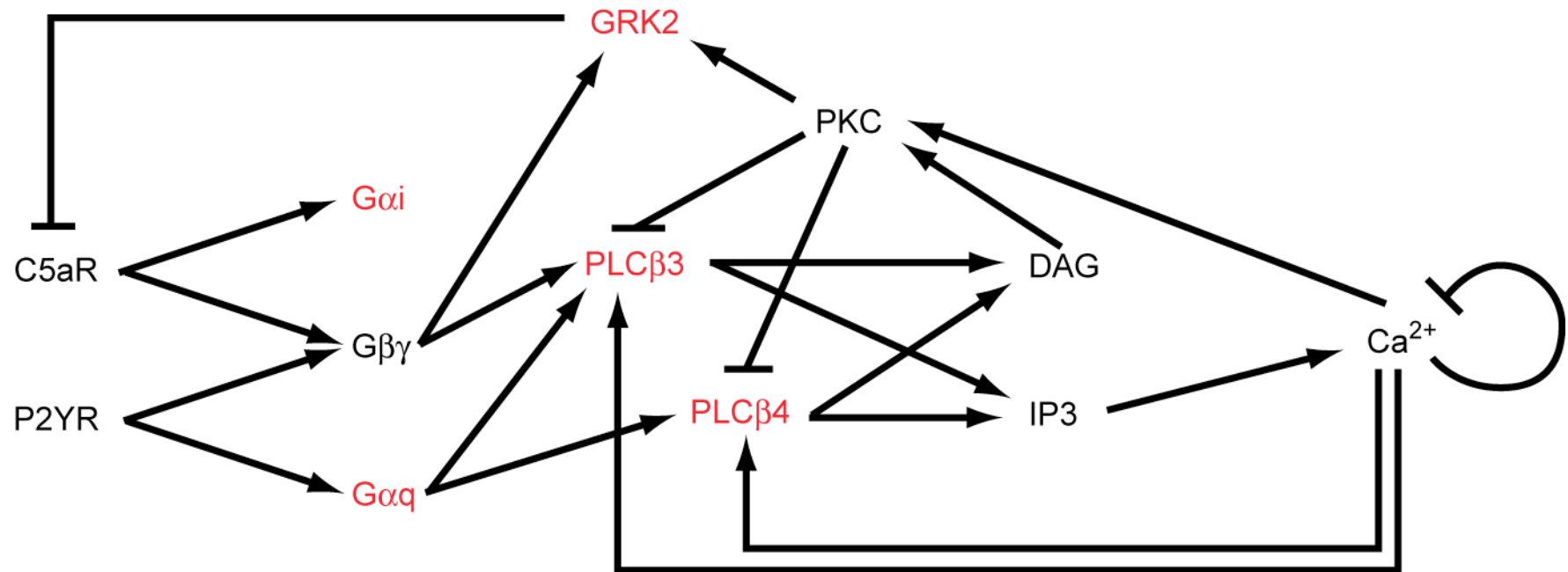
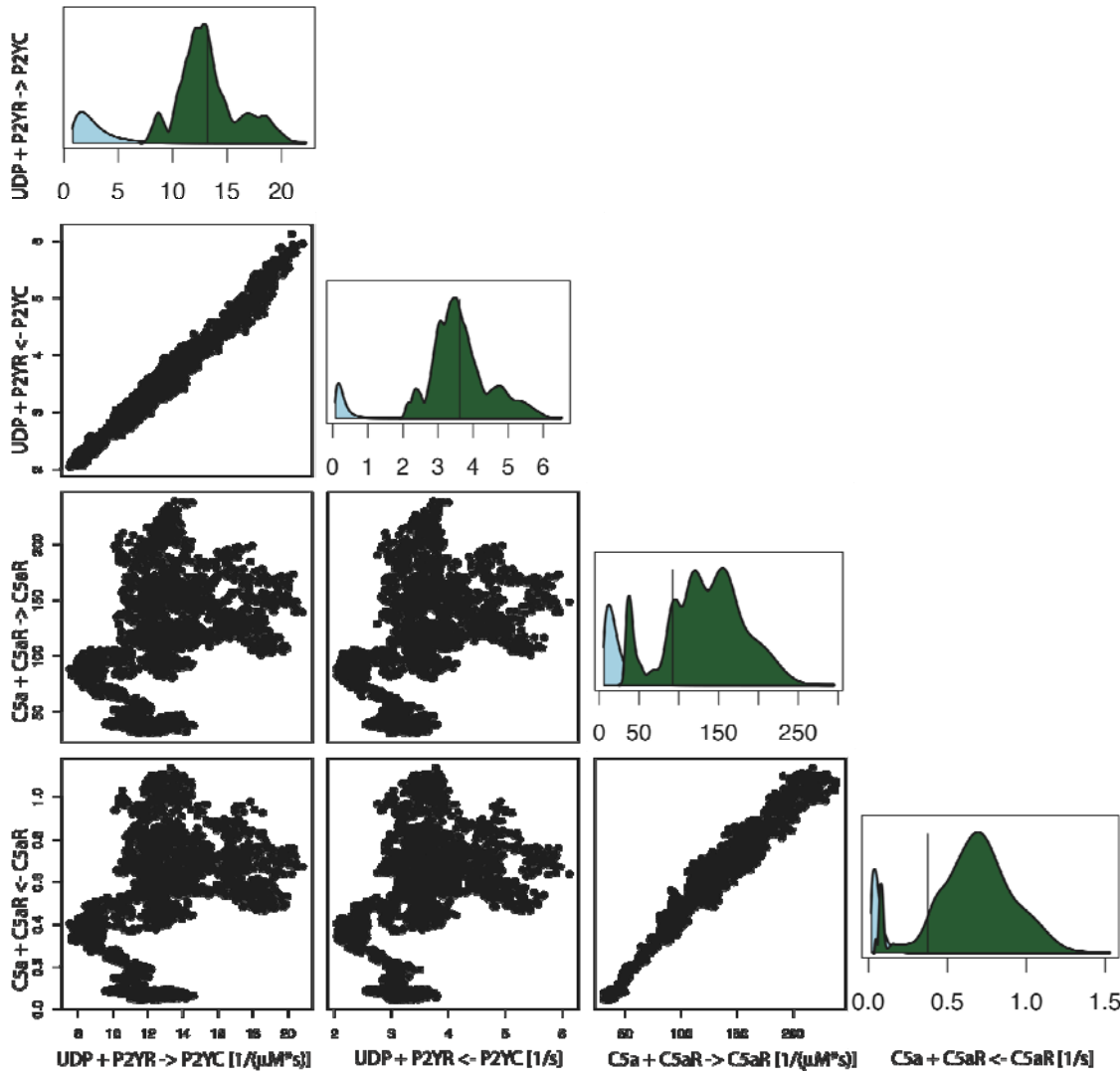
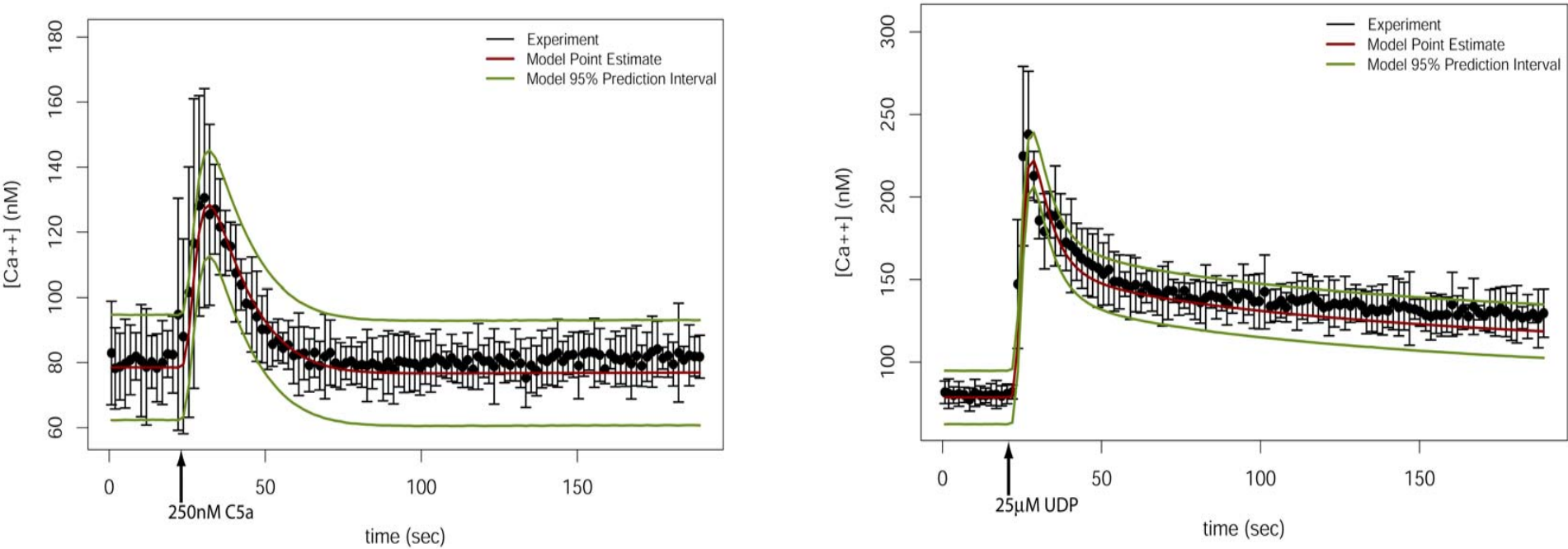


Figure 1: The model for crosstalk between the G $\alpha$ i and G $\alpha$ q pathways depends on both differential specificity and activity for G $\alpha$ i, G $\alpha$ q and G $\beta$  interactions with PLC $\beta$ 3 and PLC $\beta$ 4 to catalyze PIP2 hydrolysis and calcium dependent feedback control mediated by GRK and PKC. Selected model parameters are informed by calcium measurements taken for various ligand doses on wild-type and cell lines with shRNAi knockdowns on the proteins shown in red.

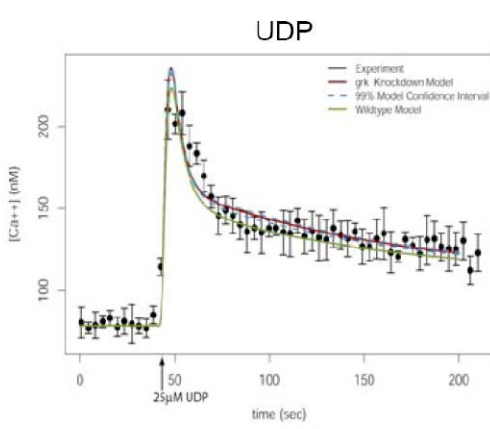
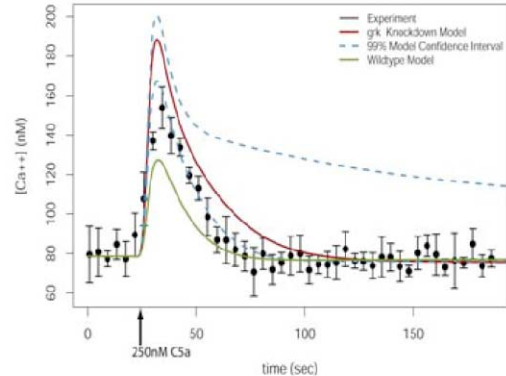


**Figure 2:** This figure shows that the single and pairwise marginal posterior distributions for the ligand binding reactions for the P2YR and C5aR receptors. The vertical line in the single marginal posterior distributions shows the point estimate that were selected. The posterior distributions show the dissociation constants for the reactions are tightly constrained by the data, while the values of the forward and reverse rates that make up the ratio are not as well constrained by the data. Additionally, as expected the UDP binding rates are not correlated with the C5a binding rates. Marginal posterior distributions for all parameters and a discussion of the point estimate selection can be found in Figure S2 (supplementary information).



**Figure 3:** Model simulations are compared to experimental data. The point estimate is computed using the posterior distribution of the parameter as estimated by Markov chain Monte Carlo given the data from 96 experiments on C5a and UDP at various doses in combination with 5 different shRNAi knockdown cell lines. The 95% posterior predictive intervals are estimated by Monte Carlo simulations including both parameter and measurement uncertainty. The measured mean and approximate 95% confidence intervals of four replicates is shown by a black dot and error bar. (left) C5a at  $250\text{nM}$  was introduced at 20s and the experimentally observed pulse in cytosolic calcium concentration is shown. (right) The qualitative shape of the calcium pulse for  $25\mu\text{M UDP}$  is different than for  $250\text{nM C5a}$ . The pulse does not completely adapt and return to the prestimulated level. For both ligands, the model prediction confidence intervals overlap the data error bars that indicate the model fit is consistent with the data within the measurement uncertainty.

## GRK Knockdown



## PLCβ3 Knockdown

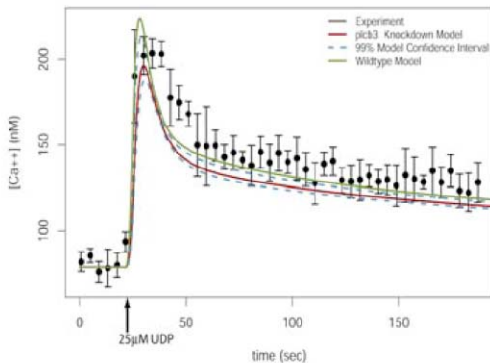
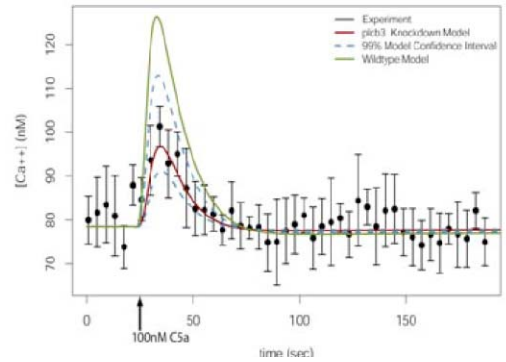
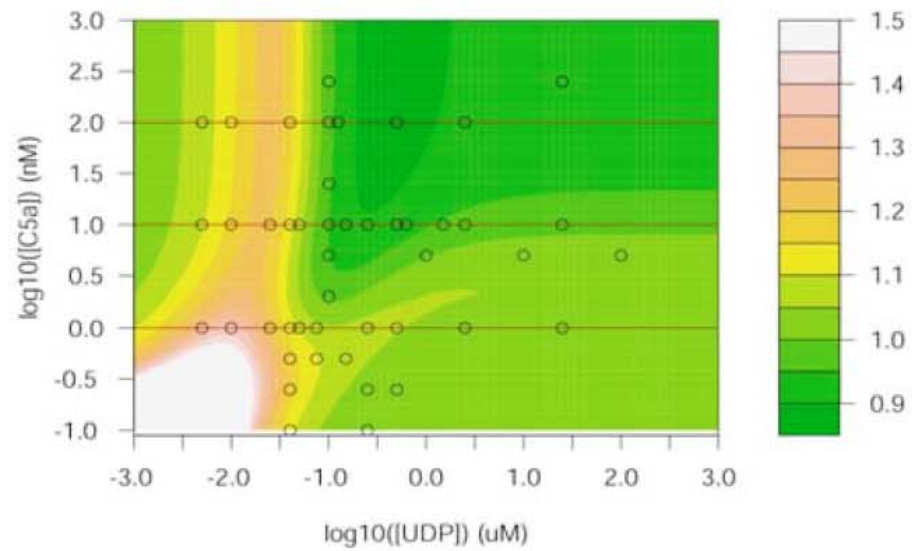


**Figure 4:** The model simulation results for GRK and PLC $\beta$ 3 knockdown cell lines stimulated with C5a and UDP are shown. The experimental mean  $\pm$  1s.d. of 3-4 replicates within one experimental run is shown in black. The knockdown simulation result with nominal knockdown fraction and parameters is shown in red and the wild-type simulation result is shown in green for comparison. Upper and lower model 99% confidence intervals (shown as blue dashed lines) are simulated using the upper and lower knockdown fraction values from Table 1. As expected the C5a response in the GRK knockdown line (upper-left panel) had an increased Ca<sup>2+</sup> response compared to wild-type. The quantitative deviation between the model and data is possibly due to the availability of multiple redundant GRK isoforms. The upper-right panel shows that the expected effect of the GRK knockdown on the UDP response is an increase in the cytosolic calcium levels. Because GRK2 does not directly desensitize the P2Y receptor in this model, the effect is likely due to a reduction of sequestration of G $\beta$  by GRK. The lower-left panel shows that the signal transduction of the C5a response is predominantly through the PLC $\beta$ 3 isoform. The effect of the PLC $\beta$ 3 knockdown is much greater for C5a than for UDP (shown in the lower-right panel).

Wild-type Synergy Ratio



GRK Knockdown Synergy Ratio

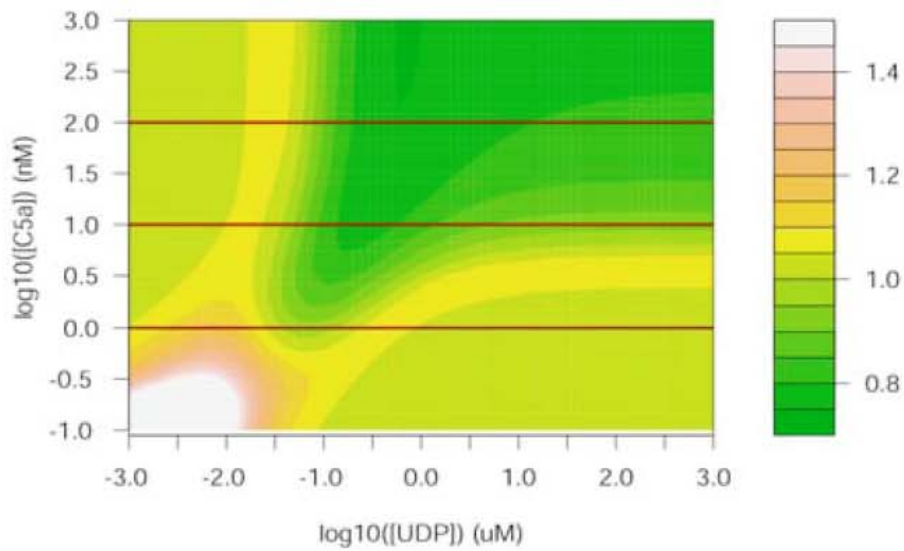


Figure 5: The model is used as a predictive tool to infer the effect of stimulating the cell simultaneously with UDP and C5a that signal through the G $\alpha$ q and G $\alpha$ i pathways respectively. Synergy was measured as the ratio of peak height offset from baseline attained from simultaneous stimulation to the peak height offset calculated by the sum of the responses to each ligand individually. The left panel shows the expected synergy ratio as a function of UDP and C5a dose (truncated at 1.5). The simulations show a ridge of synergy at a moderate UDP dose for most C5a doses. The black circles indicate dose combinations points of experiments that were conducted to test the model. The right panel shows the expected synergy ratio as a function of UDP and C5a dose for a simulated GRK2 knockdown cell line. Without the GRK-mediated negative feedback to keep the IP3 generation from the C5a receptor within the non-linear range of calcium release the ridge in the synergy dose response is diminished. The synergy in the GRK knockdown simulation is not entirely eliminated because the shRNAi knockdown of GRK does not constitute a complete loss-of-function and low concentrations of ligand are still able to synergize. Furthermore, the asymmetric synergy dose response surface is more symmetric in the GRK knockdown simulation because the asymmetric calcium-dependent feedback mechanism is reduced.